

Development of Atmospheric Monitoring System at Akeno Observatory for the Telescope Array Project

T.Yamamoto^a M.Chikawa^b N.Hayashida^a S.Kawakami^d
N.Minagawa^a Y.Morizane^b M.Sasano^c M.Teshima^a K.Yasui^b
and The Telescope Array collaboration

^a*Institute for Cosmic Ray Research, University of Tokyo, Tokyo, Japan*

^b*Department of Physics, Kinki University, Higashi-Osaka, Japan*

^c*Communication Research Laboratory, Tokyo, Japan*

^d*Department of Physics, Osaka City University, Osaka, Japan*

Abstract

We have developed an atmospheric monitoring system for the Telescope Array experiment at Akeno Observatory. It consists of a Nd:YAG laser with an alt-azimuth shooting system and a small light receiver. This system is installed inside an air conditioned weather-proof dome. All parts, including the dome, laser, shooter, receiver, and optical devices are fully controlled by a personal computer utilizing the Linux operating system. It is now operated as a back-scattering LIDAR System. For the Telescope Array experiment, to estimate energy reliably and to obtain the correct shower development profile, the light transmittance in the atmosphere needs to be calibrated with high accuracy. Based on observational results using this monitoring system, we consider this LIDAR to be a very powerful technique for Telescope Array experiments. The details of this system and its atmospheric monitoring technique will be discussed.

Key words: Cosmic Ray, Fluorescence Technique, Atmospheric Monitoring

1 Introduction

The air fluorescence technique for air shower observation has many advantages, (for example, direct measurement of shower longitudinal development, and stereo geometrical reconstruction with multiple eyes). These advantages will bring technical breakthroughs in EHE Cosmic Ray physics.

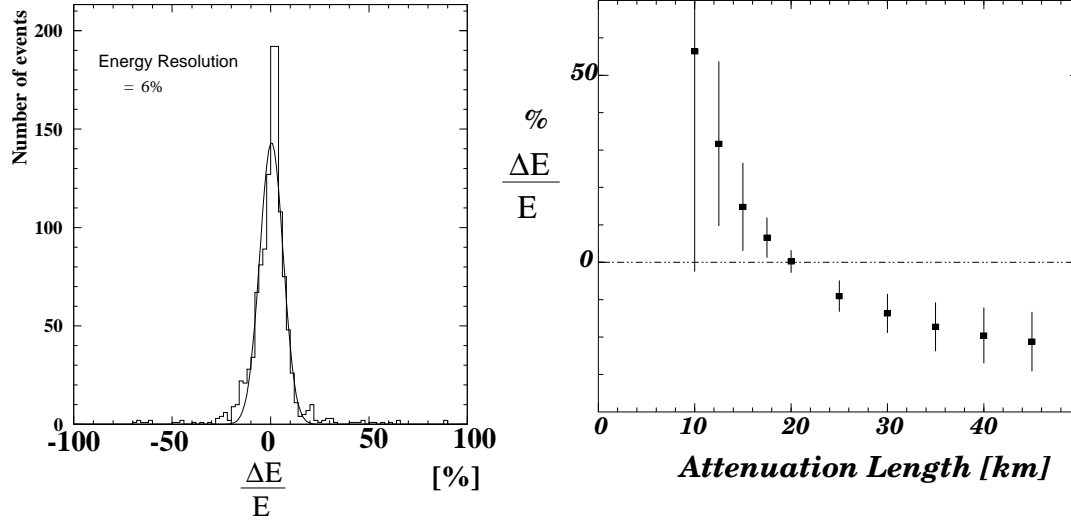


Fig. 1. Results of Monte-Carlo simulation for the Telescope Array. Left panel indicates the energy resolution of the Telescope Array for 10^{20} eV cosmic rays. The energy resolution is better than 6% in 1σ as long as we know the transmittance of the atmosphere. Right panel shows the error of estimated energy for 10^{20} eV cosmic rays as a function of incorrectness of atmospheric correction of attenuation length. The values used for the simulation were $L_M = 20\text{km}$ and $H_M = 1.2\text{km}$.

On the other hand, this fluorescence technique has a serious problem. In this technique the light yielded from air showers after the transmission is measured in atmosphere at a $10 \sim 60$ km distance. Atmosphere can be considered a part of the detector. Without any monitoring, the atmospheric conditions may cause large uncertainty in the experiment and result in serious systematic error. Therefore, the calibration of the light transmittance in the atmosphere is essential for the air fluorescence experiment.

Charged particles in the air shower excite air molecules and yield fluorescence light of between 330nm and 400nm. This fluorescence light is also scattered by molecules and aerosols in the air before it reaches the detector. The scattering process caused by molecule is called Rayleigh scattering. The attenuation length of this scattering process X_r is 2974 g/cm^2 for a 400nm wave length. Amount of scattered photons with wave length of λ can thus be calculated by following equation

$$\frac{dN_r}{dl} = -\rho \frac{N_r}{X_r} \left(\frac{400\text{nm}}{\lambda} \right)^4 \quad (1)$$

where ρ is the atmospheric density. In this equation, the number of scattered photons is proportional to λ^{-4} . This scattering process seriously effects the observation of fluorescence light in the air.

For example, when we consider the typical measurement of fluorescence light

from an air shower at a distance of 30 km from detector, with a detector altitude of 1.5km and an elevation angle of 30 degrees, the fluorescence light has to pass through about 2200 g/cm^2 in the air and 70% of the photons will be scattered by this Rayleigh process.

There is another scattering process, Mie scattering. There are many kinds of scattering materials in the atmosphere, such as, water vapors, mists, clouds, dusts, blown small sands, artificial fumes, exhaust gas from cars, and smoke from forest fires. Furthermore, 'Kosa' from the Gobi desert in China is spread over a wide area of the northern hemisphere. These atmospheric aerosol's densities and their components change significantly with location and time. The scattering of photons by these aerosols is called Mie Scattering. In the Utah desert, the typical scale height of Mie scattering H_M is 1.2 km and horizontal attenuation length L_M is 20 km. The amount of scattering photons can be expressed by the following equation

$$\frac{dN_r}{dl} = -\frac{N_r}{L_M} \times \exp\left(-\frac{h}{H_M}\right) \quad (2)$$

Therefore, under the previously described conditions, approximately 27% of the photons contained in the fluorescence light from the air shower are scattered by the Mie process. When we take into account Rayleigh and Mie scattering, about 22% of the photons can reach our detector.

The Telescope Array (TA) will observe the air showers which flash far from the detector, for example, at more than 50km. Figure 1 shows the results of Monte-Carlo simulation for TA. According to this simulation study, the energy resolution of TA is better than 6% if atmospheric transmittance is accurately taken into account. However, if we apply the 20% shifted value in the attenuation length, the estimated cosmic ray energy has a systematic error of nearly 10%. To estimate the primary composition, TA will use X_{max} which is the maximum position in the longitudinal shower development. The intrinsic resolution of X_{max} is estimated to be 20g in the TA experiment using Monte Carlo simulation. If the assumed attenuation length differs by 20%, we estimate X_{max} with a 10g systematic error. The correction of atmospheric transmittance affects not only energy determination but also air shower reconstruction. To realize this high resolution power of TA, we need to measure the attenuation length of the atmosphere with an accuracy of a few percent or better.

For the purpose of the atmospheric monitoring, TA and High Resolution Fly's Eyes are developing various methods which use a laser or flashers[1][2][3][4][5]. One of well-known technique for atmospheric monitoring is LIDAR which has been developed for environmental science. Using this technique, atmospheric conditions can be monitored remotely by measuring back-scattered light from

a pulsed laser beam.

We are developing a steerable LIDAR system to study the atmospheric monitoring method in Akeno Observatory. In the present paper, we will describe the details of this system and discuss how to accurately measure transmittance in the atmosphere.

2 LIDAR equation

In general, the intensity of the back-scattered light detected by LIDAR is expressed by the following equation (LIDAR equation)

$$P(R) = \frac{P_0 \kappa A (c\tau/2) \beta(R) T^2(R) Y(R)}{R^2} + P_b \quad (3)$$

where

$P(R)$: intensity of the detected light

P_0 : laser intensity

P_b : intensity of back ground photons

c : light velocity

R : distance from laser to target

τ : integration time

$Y(R)$: geometrical efficiency of the beam track and receiver

A : aperture of receiver

κ : detector efficiency

β : back-scatter coefficient

$T(R)$: transmittance ($= \exp(-\int_0^R \alpha dr)$)

α : extinction coefficient ($=1/\text{attenuation length}$)

We define the following parameters for convenience

$$P_0 \kappa A \frac{c\tau}{2} Y(R) \equiv C \quad (4)$$

$$X(R) \equiv R^2(P(R) - P_b) \quad (5)$$

$$S(R) \equiv \ln(X(R)) \quad (6)$$

The LIDAR equation can be then written as follows:

$$X(R) = C \beta(R) T^2(R) = C \beta(R) \cdot \exp(-2 \int_0^R \alpha dr) \quad (7)$$

If α is constant until R ,

$$X(R) = C\beta \exp(-2R\alpha) \quad (8)$$

Then we obtain the differential LIDAR equation

$$\frac{dS(R)}{dR} = \frac{1}{\beta(R)} \frac{d\beta(R)}{dR} - 2\alpha(R) \quad (9)$$

There are two variable parameters in this LIDAR equation. One is the extinction coefficient α that represents the amount of scattered photons in a scattering volume. This value corresponds to the reciprocal of attenuation length. The other variable parameter is the back-scattering coefficient β that represents the amount of scattered photons in the backward direction. This value is proportional to the density of scattering matter and its differential cross-section. Since the LIDAR equation has two variables, it can not be solved in general.

If the atmosphere is uniform, β is constant and $d\beta/dR = 0$. Then

$$\alpha = -\frac{1}{2} \frac{dS}{dR} \quad (10)$$

Thus we can measure the α using this equation.

If we assume a relationship between α and β , the variable parameters can be reduced. For this purpose, an empirical relationship is proposed as follows:

$$\beta = \text{const} \cdot \alpha^k \quad (11)$$

In this assumption, k depends on the atmospheric condition and wave length of the laser. It is empirically estimated to be 0.6~1.0. Substituting this relationship into equation(9), we obtain

$$\frac{dS}{dR} = \frac{k}{\alpha} \frac{d\alpha}{dR} - 2\alpha \quad (12)$$

This is a Bernoulli-type equation.

Vieze adopted the boundary condition near the detector and obtained the following solution[6].

$$\alpha(R) = \frac{X(R)^{1/k}}{\frac{X(R_c)^{1/k}}{\alpha(R_c)} - \frac{2}{k} \int_{R_c}^R X^{1/k}(r) dr} \quad (13)$$

Since the second term of the denominator is negative, the denominator approaches zero with an increase of R . This solution often diverges, and is unstable.

Klett proposed a stable solution by adopting the boundary condition at the farthest point R_c , and obtained following solution[7]

$$\alpha(R) = \frac{\exp[(S(R) - S(R_c))/k]}{\alpha(R_c) + \frac{2}{k} \int_R^{R_c} \exp[(S(r) - S(R_c))/k] dr} = \frac{X(R)^{1/k}}{\frac{X(R_c)^{1/k}}{\alpha(R_c)} + \frac{2}{k} \int_R^{R_c} X^{1/k}(r) dr} \quad (14)$$

In this solution, the integral term of the denominator becomes larger with R . Thus the contribution of uncertainty of the critical value $\alpha(R_c)$ becomes smaller. Therefore this solution converges on the correct value. Using Klett's method, we can analyze α , if we can assign certain values to the parameter ' k ' and the critical value $\alpha(R_c)$.

Furthermore, Fernald proposed a similar solution which considered atmospheric compositions[8]. This solution assumes that $k = 1$ and that scattering parameter $S_a \equiv \alpha_M/\beta_M$ is constant. Then α can be analyzed in successive steps using the Klett method. After the invention of these methods, analysis of the LIDAR signal based on elastic scattering made rapid progress.

3 Experiment

Wave length[nm]	1064	532	355	266
Pulse Width[nsec]	6-8	5-7	4-6	4-6
Energy [mJ]	50	25	7	5
Pulse Repetition Rate [Hz]	10	10	10	10
Beam Diameter [mm]	2.75	2.5	2	2
Beam Divergence [mrad]	3	3	2	2

Table 1

The laser's specification. This laser is a flash-lamp pumped, Q-switched, and water cooled Nd:YAG type. At present we use a 355nm wave length.

The steerable LIDAR system was developed at Akeno Observatory in Yamanashi Prefecture, Japan; its geographical coordinate is 900m a.s.l., 138.5°N, 35.78°E. This observatory utilizes are many cosmic ray detectors including AGASA and fluorescence detectors. Using these detectors, hybrid observation of cosmic rays are performed.



Fig. 2. Akeno Steerable LIDAR System

This LIDAR system is situated on the roof of the Akeno Main laboratory. All of the devices are housed in the astronomical dome shown in Figure 2. This astronomical dome consists of a cubic-shaped room of $1.8\text{mW} \times 1.8\text{mD} \times 1.0\text{mH}$ and a steerable dome. The dome window can open to 1m , and its direction must be rotated according to the movement of the laser. Two motors are

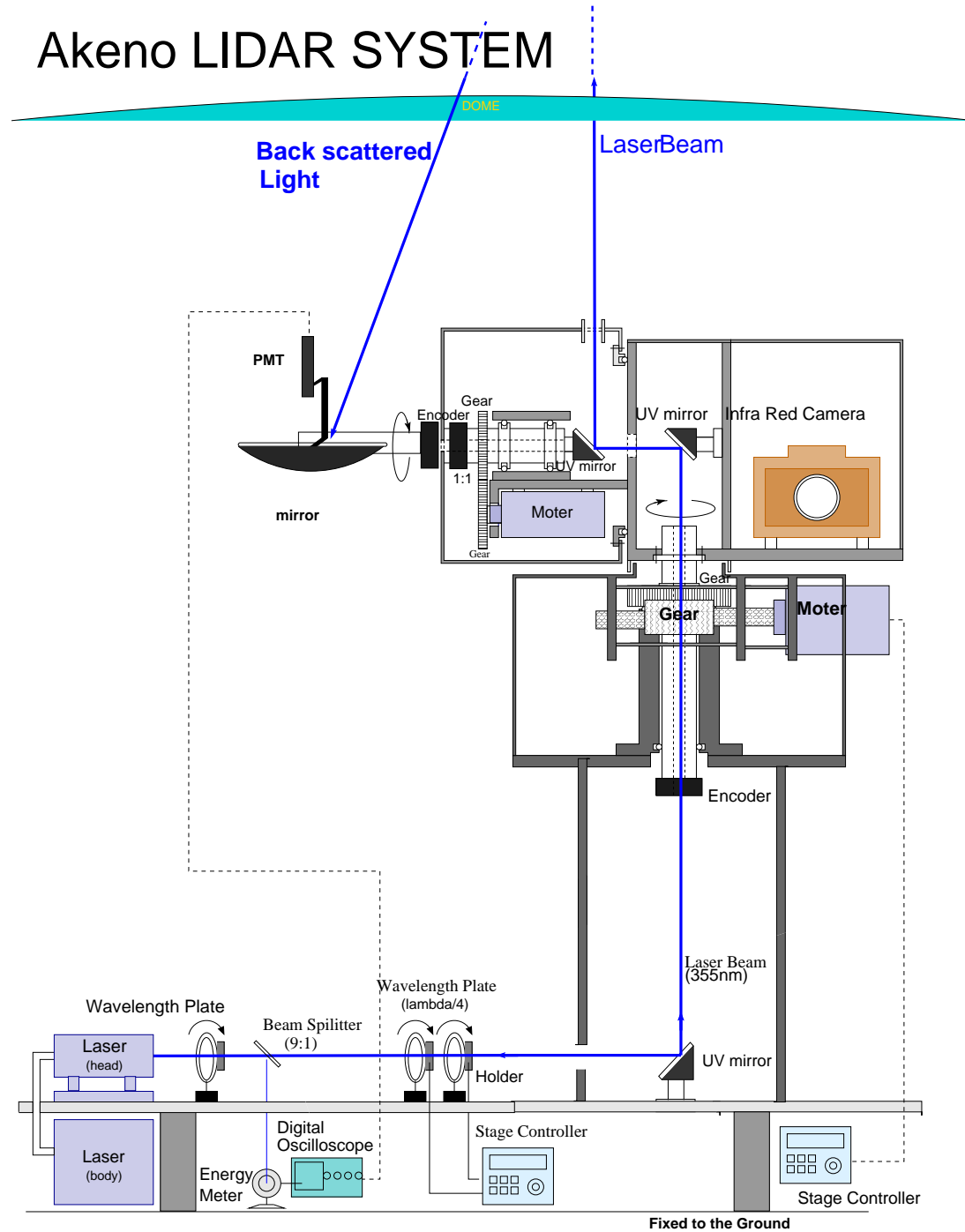


Fig. 3. Diagram of the steerable LIDAR system developed at Akeno observatory. equipped for opening and closing the dome and for dome rotation. Each motor is controlled by an electronic switch which operated by a local computer.

The steerable LIDAR system is illustrated in Figure 3. Inside the dome, laser and optical devices are installed on an optical table which is fixed on the concrete pad. This laser is a flash lamp pumped, Q-switched, and water cooled

Nd:YAG type. Its specifications are shown in Table 3. The third harmonic beam with a wavelength of 355nm is used in this experiment. This wavelength is close to the major lines of air fluorescence light. The maximum beam intensity is 7 mJ and its maximum repetition rate is 10 Hz. The beam intensity, repetition rate, and shooting duration can be controlled by the computer through RS232C.

The laser beam is split into two directions after phase conversion by the circular polarizer. One has 10% intensity which is used for energy calibration, while the other 90% is transported to the shooting system. To stabilize the laser and to prevent condensation, these optical devices including the laser and the optical table are isolated from the outside atmosphere by a fireproof curtain and the temperature is kept constant by an air conditioner.

An alt-azimuth mount is adopted for the shooting system. Encoders are directly mounted on each axis. The resolution of these encoders is 5/1000 degrees. Each axis is driven by AC stepping motors with 0.0072 degree steps. The maximum speed of this shooting system is more than 10 degrees/sec.

An infrared camera is also mounted on the azimuthal axis. Using this infrared camera, clouds can be recognized as hot regions in the cool night sky. The typical cloud temperature is higher than a few degrees; however, the typical night sky temperature is lower than -10 degrees. This infrared camera can measure the temperature between -20 and 20 degrees and its field of view is 20×40 degrees. To increase the data rate, the video image from this camera is captured as a ppm format image file through a VIDEO capture board.

Two mirrors are mounted on the elevation axis. One is a shooting mirror for the laser beam. The other is a receiving mirror for back-scattered light. Maximum beam intensity shot to the sky is about 5 mJ. The receiving mirror is adjusted to parallel the laser beam. A parabolic mirror of 16 cm in diameter is adopted for this receiving system. Because the shooting and receiving mirrors are mounted on the same part, the laser beam and the receiver can be moved simultaneously. A one-inch PMT is located at the focus of 16cm diameter mirror. The field of view is about 1 degree. PMT gain is adjusted to about 10^6 . The signal from the PMT is acquired by a 100MHz band-width Digital Oscilloscope (TDS33014 made by Tektronix cooperation) which measures the time profile of the back-scattered light. The time range of the signal sweep is set to $10\mu\text{sec}/\text{DIV}$ and one sweep consists of 500 wards with a time resolution of 200nsec. Since the timing of the back-scattered light in the LIDAR system corresponds to the round-trip time to the target, 200nsec time resolution is equivalent to 30m in spatial resolution ΔR . When we set 1 bit to 0.4mV (it corresponds to 10mV/DIV with 256 bits digitizer), then 1 bit corresponds to about 2 photo-electrons. An average of 16 shots is calculated by this oscilloscope and recorded on the local computer.

All of these systems are controlled by the local computer using a Linux operating system and operated by the remote computer via a network.

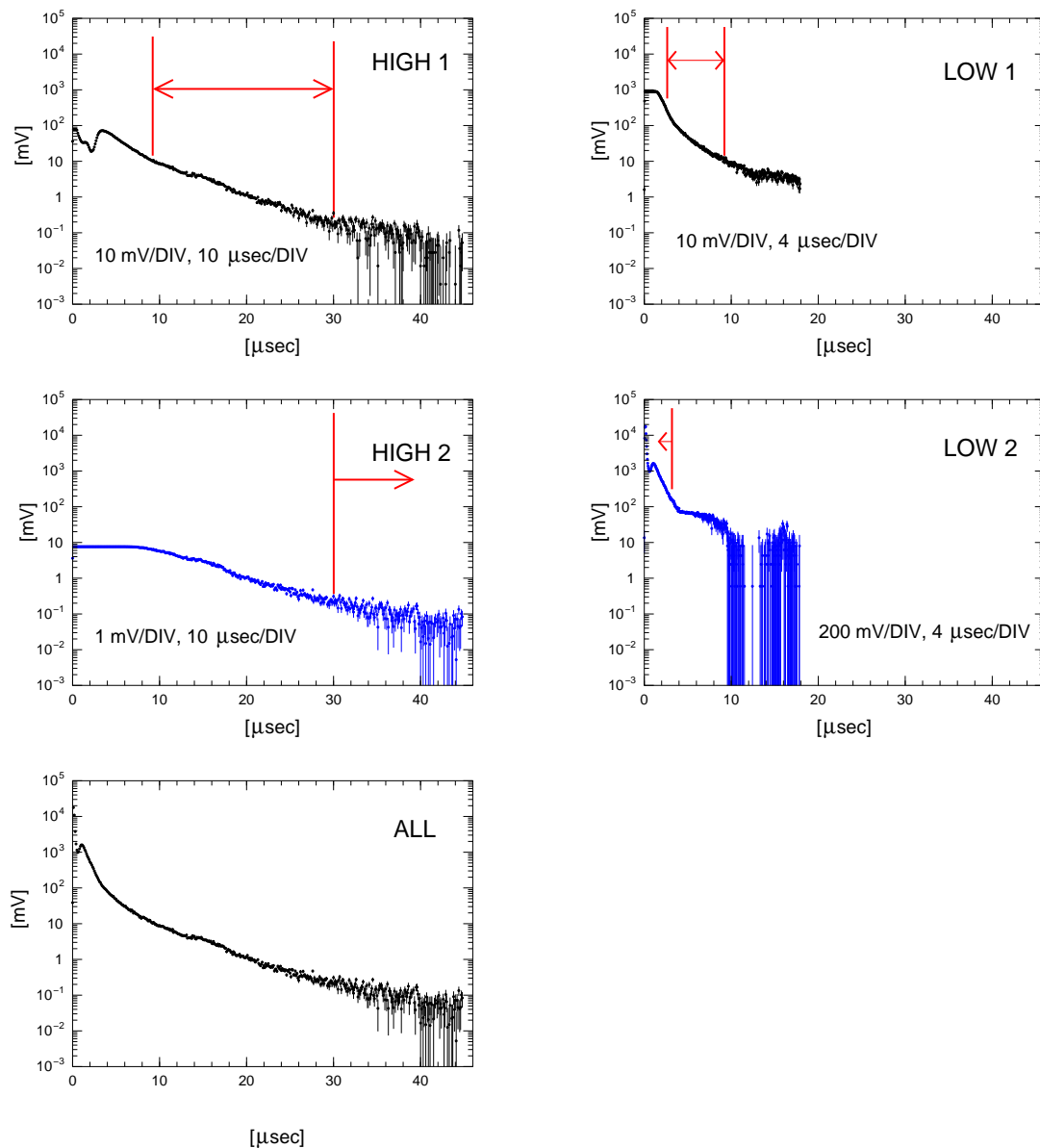


Fig. 4. Example of a time profile of one direction. An average of 1024 shots in the vertical direction are plotted. To increase dynamic range, we use two channels: high sensitivity channels (left panels) and low sensitivity channels (right panels). Laser intensity is 5mJ for the high sensitivity channel and 0.4mJ for the low sensitivity channel. The amplitude of the low sensitivity channel is normalized by laser intensity. Each channel is measured in two oscilloscope ranges as indicated in each panel. The regions indicated by dashed lines are used for the analysis. The lower panel indicates the average of the four channels.

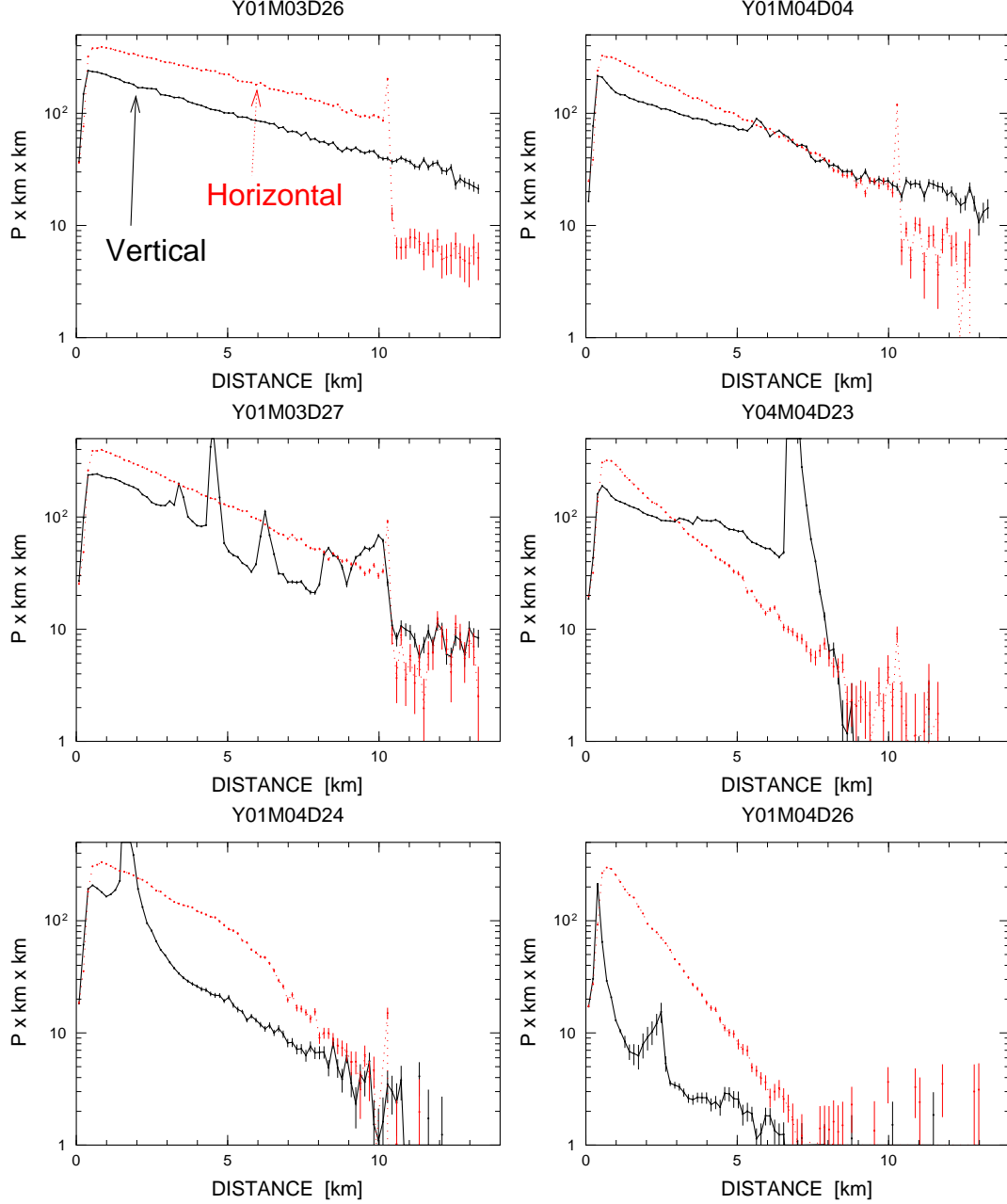


Fig. 5. X-axis is the distance from the laser. Y-axis is the pulse height multiplied by the square of the distance ($X(R)$). Dotted lines indicate the horizontal measurement. Solid lines indicate vertical measurement. The upper left panel shows a result obtained on a clear night. The lower right panel shows a result obtained on a cloudy night.

4 Observation

The Telescope Array is planned to build 10 stations with 40km separation in the Utah desert USA. The location of those stations will be spread over a

very wide area, their operation should be done remotely via a network linked by microwave or optic fiber. This would constitute a severe constraint for our atmospheric monitoring system. For this reason, we developed a fully automated system at Akeno observatory. For example, if it begins to rain during the observation, the system is shut down automatically.

The intensity of the back-scattered light reaching the detector from a scattering point is proportional to the inverse of the square of the distance, the density of the atmosphere, and the intensity of the laser beam. For this reason, the amount of returned light from near the detector is huge and that from a distant point is faint. Therefore a very wide dynamic range, typically 4 orders of magnitude, is required for the light receiving detector. If we use a high intensity laser beam, the PMT is saturated by photons scattered near the detector. If it is weak, the number of measurements have to be increased in order to measure the signal from a distant place, thus lengthening the observation time.

To increase the dynamic range, we use low and high sensitivity channels. Each channel uses two settings on the digital oscilloscope as illustrated in Figure 4. For the high sensitivity channel, the laser beam is shot at 5 mJ into the sky and oscilloscope ranges are adjusted to 1mV/DIV and 10mV/DIV. In this case, the PMT is saturated by scattered photons near the detector and it takes more than 9 μ sec to recover sensitivity. Data points with signal amplitudes of less than 2 mV are not used in the analysis in order to obtain a reasonable signal to noise ratio, and to reduce the uncertainty of the pedestal. This value corresponds to about 1 p.e., i.e., 5 bits for 1mV/DIV. For the low sensitivity channel, the laser intensity is reduced to about 1/12 and the oscilloscope ranges are adjusted to 10mV/DIV and 200mV/DIV. In this case, the PMT recovers by 8 μ sec. Using this channel, we can measure the back-scattered light from a distance between 1.2 km and 3 km.

The signal profiles of 16 shots are averaged by the digital oscilloscope and then recorded on the local computer. This measurement is repeated 48 times in vertical and horizontal directions and 16 times for every 5 degrees between 85 and 5 degrees. In other words, 1024 shots are measured in the vertical and horizontal directions, and 256 shots are measured in other directions.

Examples of measurements are shown in Figure 5. In this figure, the results in the vertical and horizontal directions are shown. In the horizontal measurement, if the atmosphere depends on only altitude (meaning that the atmosphere has a 1-D structure and is uniform), $S(R) \equiv \log(X(R))$ is in proportion to R and extinction coefficient α is analyzed in terms of the slope using equation(10). If the atmosphere is not uniform in the horizontal direction, the slope is not constant, depending on the atmospheric conditions. We can see $S(R)$ decline linearly to 10 km under good weather conditions as shown in

Figure. There is a mountain at a distance of 10km and the light scattered by this mountain can be seen in this figure. The atmosphere is not uniform under bad weather and $S(R)$ does not decline linearly. In measurements in the vertical direction, it can be clearly seen that clouds cause the magnitude of the signal strength to vary rapidly. We can measure the atmosphere up to an altitude of 12km under a clear sky.

5 Analysis

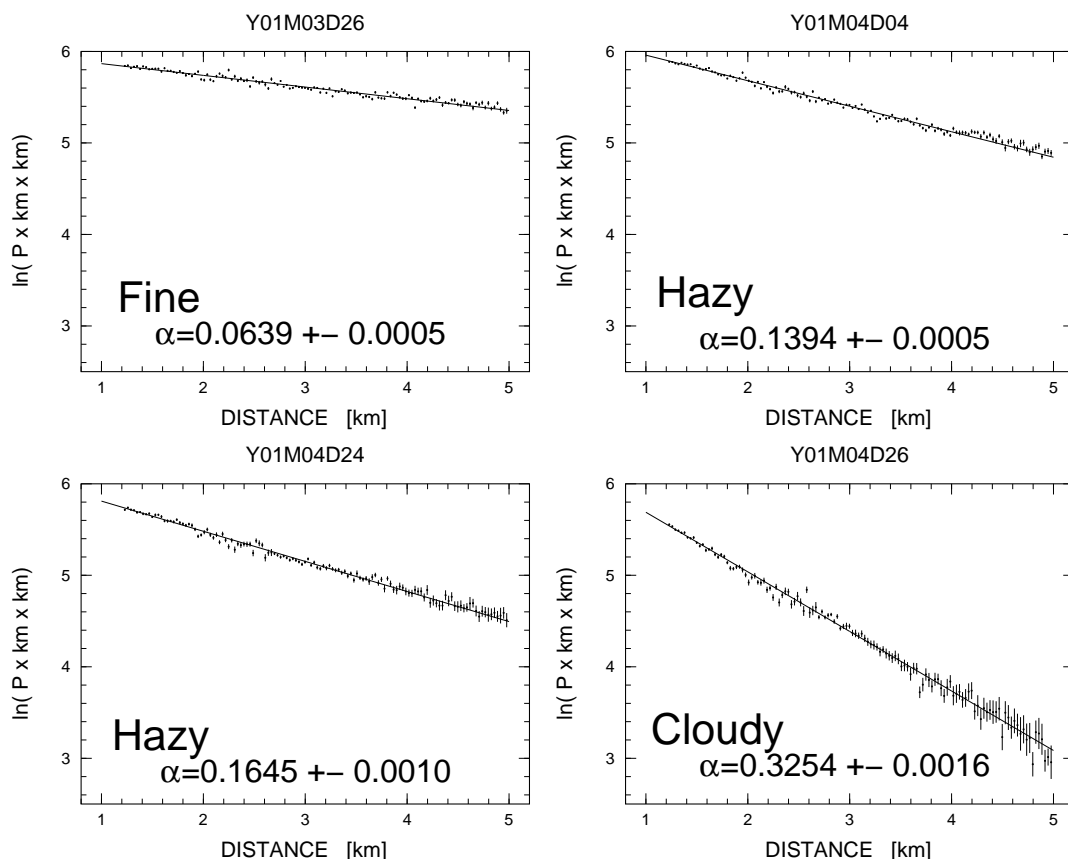


Fig. 6. Example of horizontal measurement. Regions from 1.2 km to 5 km are plotted. The upper left panel represents the clearest night, and the lower right panel represents a cloudy night. Solid line is result of fitting by straight line. The extinction coefficient α can be estimated using the slope of this line. The estimated α is indicated in each panel.

In this section, we discuss how to estimate the transmittance of the atmosphere using the results of the measurements described above.

One of the simplest cases is horizontal measurement. If the atmosphere is uniform, α can be analyzed using equation(10) at the level of the detector

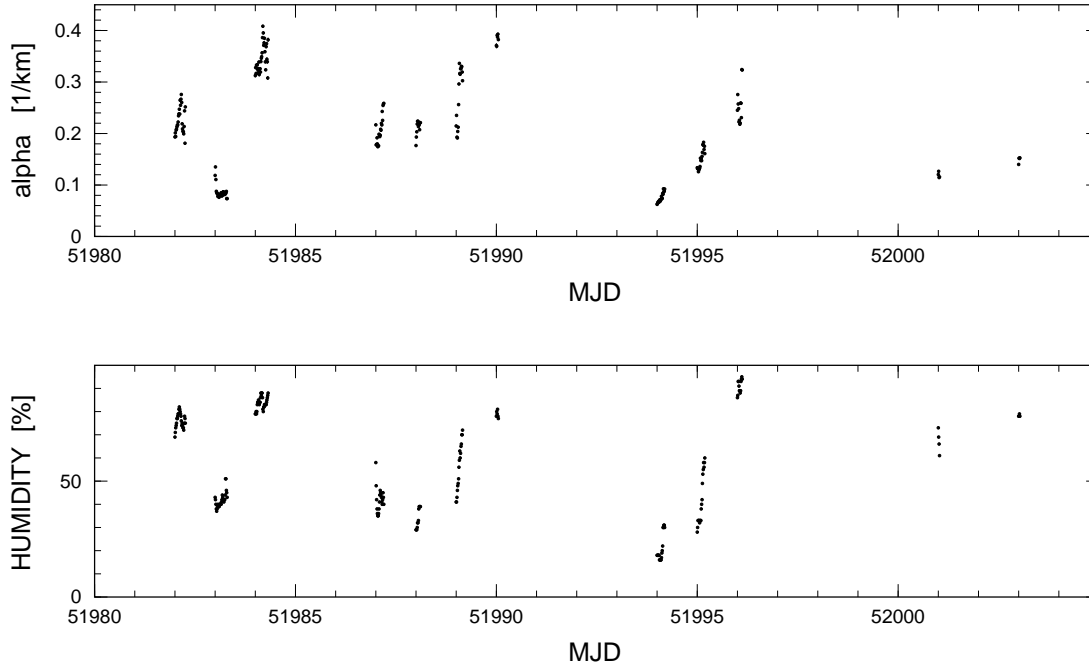


Fig. 7. Upper panel shows estimated α at the level of the detector as a function of observation time. Lower panel shows humidity measured simultaneously.

as mentioned previously. Figure 6 shows examples of this horizontal measurement. Data which is comparatively near the detector is used. It can be seen that the attenuation of the laser beam clearly depends on the weather. It can also be confirmed that the atmosphere is uniform in this region. Figure 7 shows the time profile of α in comparison with humidity which is measured simultaneously. Of course, the transmittance of the atmosphere depends not only on humidity; however, in this figure we can see that variation of α follows tiny variations of humidity. This method appears to be very convincing and accurate.

As described section 2, the LIDAR equation cannot be solved because it has two variable parameters. A solution which uses an assumption of the empirical relationship between α and β is proposed by Klett. To estimate α using Klett's method, we need to determine two parameters: one being the critical value at the highest altitude point, the other being parameter k which represents the relationship between α and β . To determine these parameters, we use a simple assumptions as follows:

- In a measurement in the vertical direction, the smallest α corresponds to the value expected from Rayleigh scattering. If there are no clouds, this value can be estimated at its highest point.
- In a measurement in a different direction, a smaller α (meaning the value in a cloudless region) corresponds to the α which is measured at a direction of +5 degrees at the same altitude.

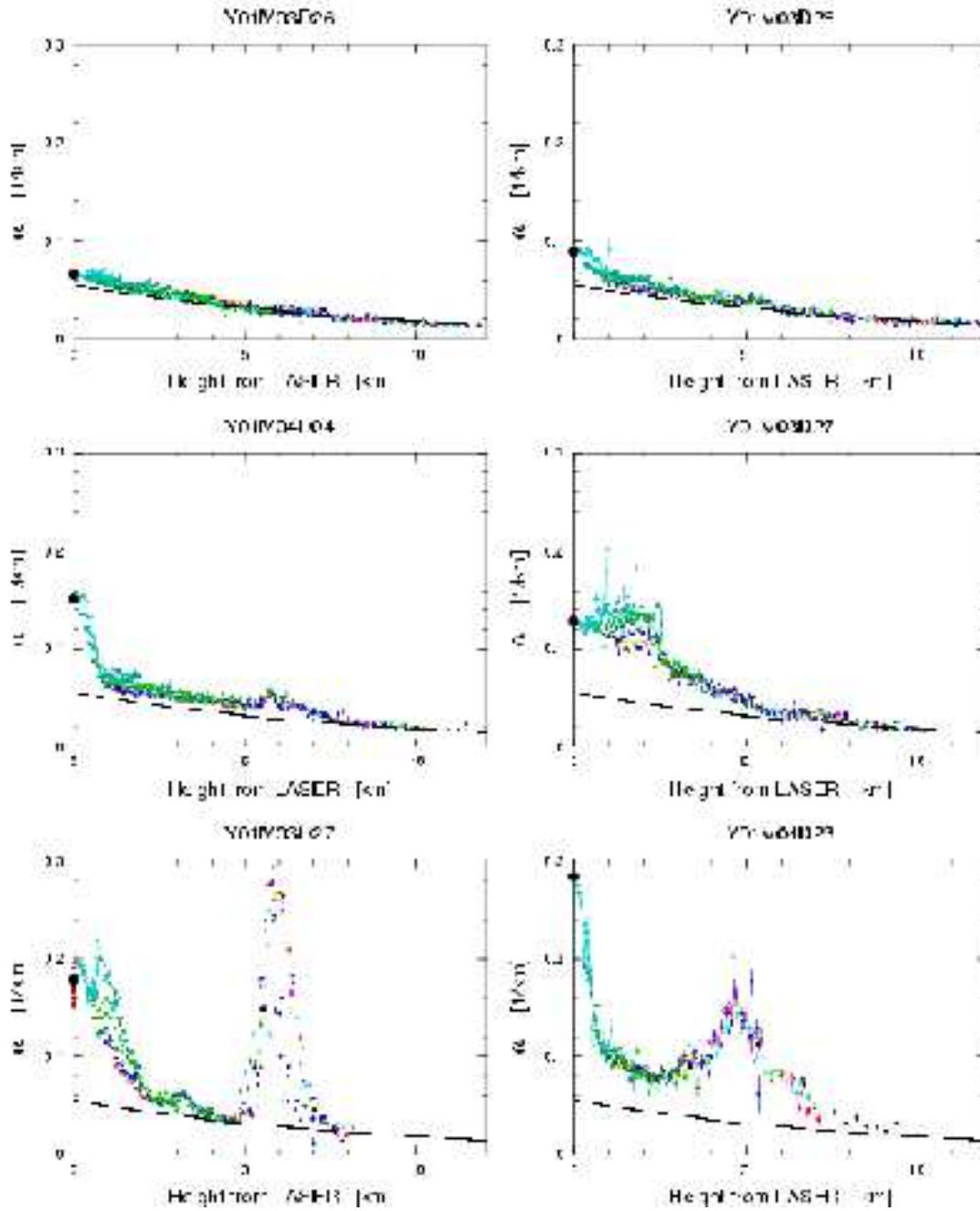


Fig. 8. Estimated α using Klett's method as a function of altitude. Different colors correspond to different zenith angles. Solid lines indicate the expected value from Rayleigh scattering. Black dots at height 0 indicate the measured value in horizontal shot. The upper left panel shows the results of the clearest night. The lower left panel shows a cloud at around 6km altitude. This cloud obscures the signal from a higher altitude. Because the boundary condition cannot be determined, the absolute value cannot be analyzed correctly.

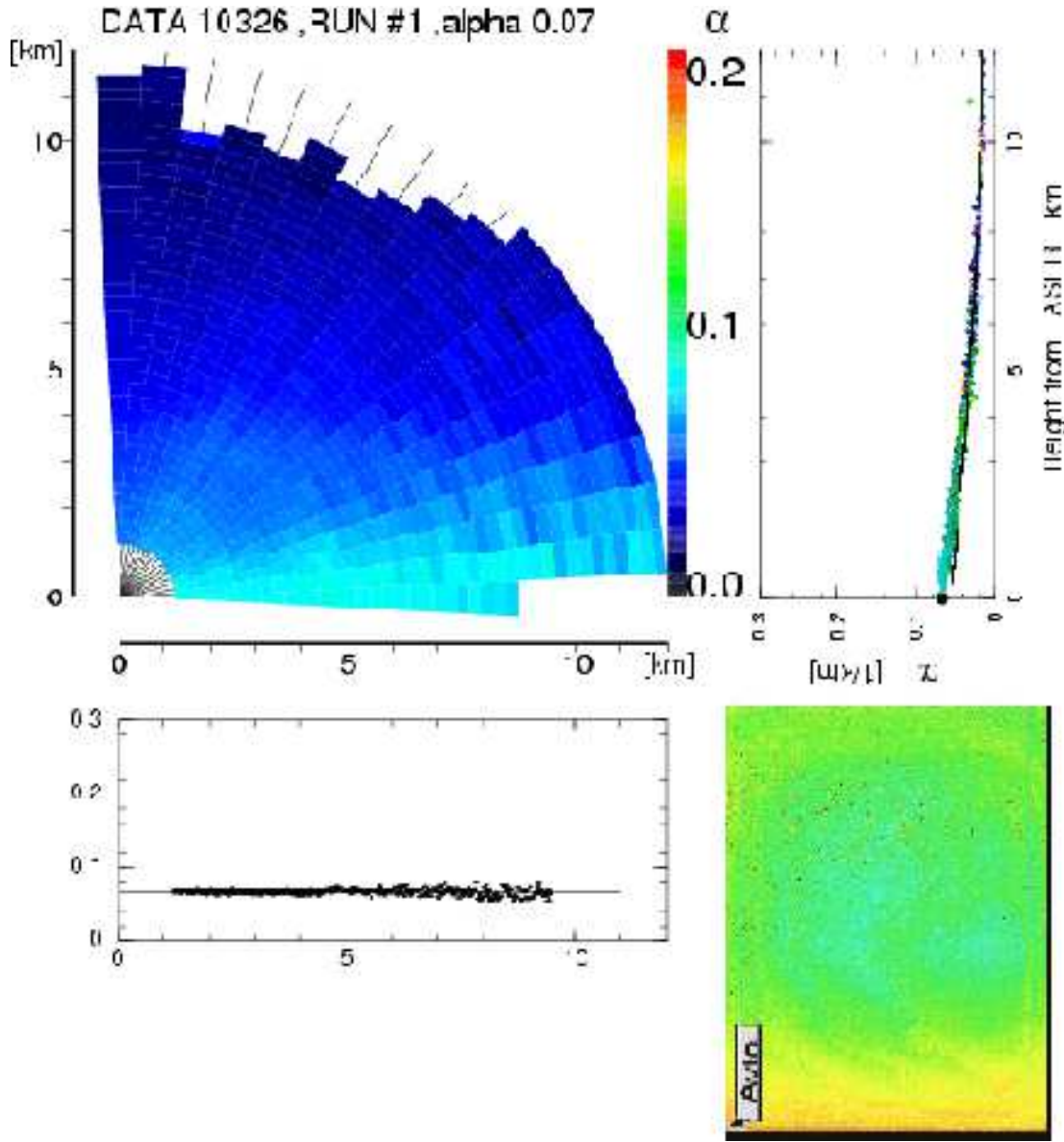


Fig. 9. An example of estimated extinction coefficient α . The upper left panel shows a two-dimensional map of α inside a 12 km radius circle with LIDAR in its center. Estimated α in horizontal measurement is indicated above this panel. The upper right panel is the same as that in the previous figure. The lower left panel shows the estimated extinction coefficient in horizontal shots. The solid line indicates the result of fitting. The lower right panel shows an image taken by the infrared camera. This data regards the clearest night.

- α at points lower than 100m can be estimated by the α obtained in the horizontal measurement.

In the first assumption, we estimate the critical value based on Rayleigh scattering. This means that we assume the atmosphere is clear and the effect of Mie scattering can be ignored at high altitudes, which is about 10 km with the

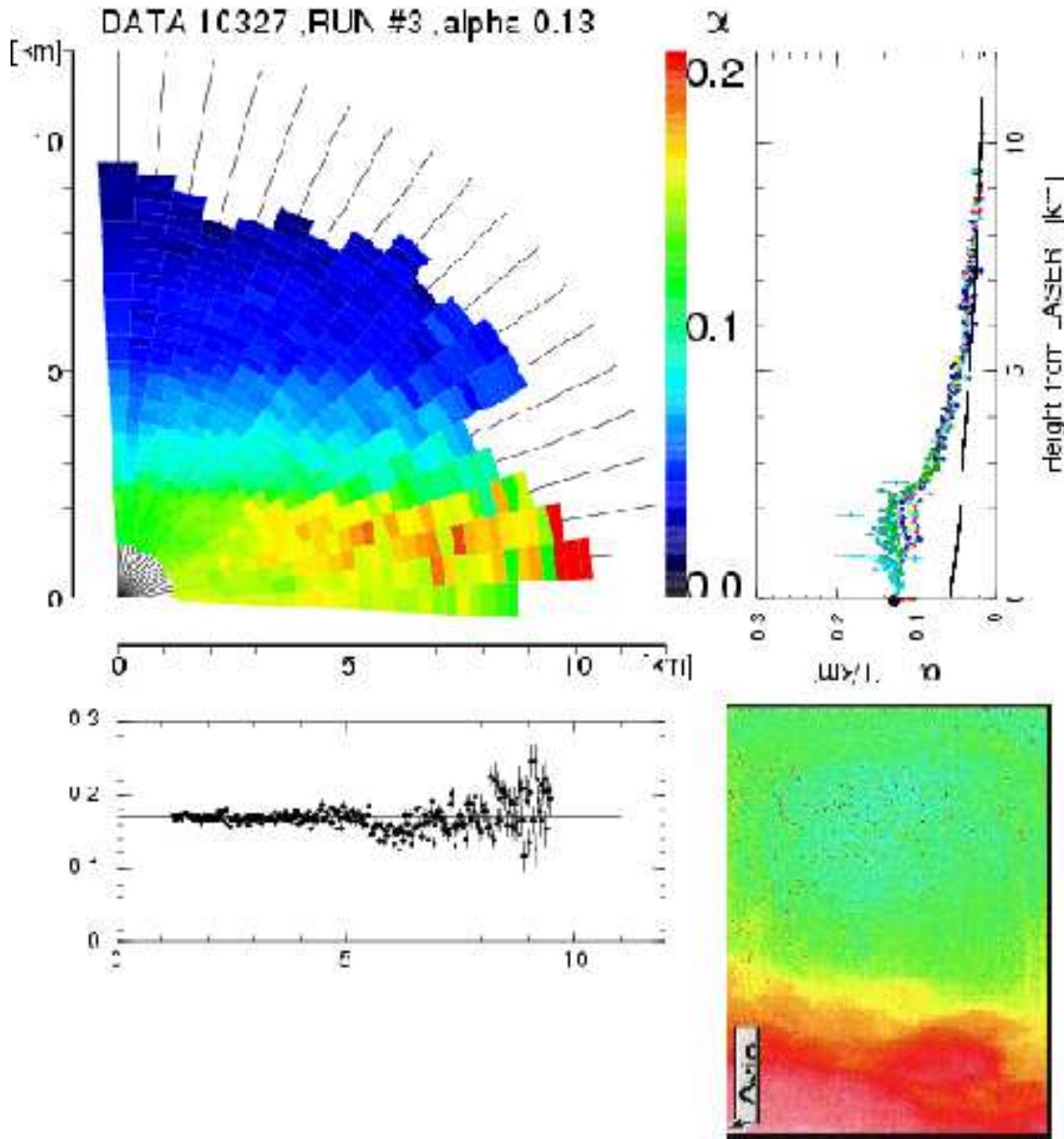


Fig. 10. Data of the next night. The expression is the same as in the previous figure. The atmosphere was hazy at low altitudes.

present system. Transmittance is analyzed in successive steps from the critical point to the lower point. For this reason, errors in the critical value affect the measurement of the lower points. This assumption is reasonable during good weather conditions. However, if the weather is not clear, this assumption causes significant systematic error.

At small elevation angles, it became difficult to measure the transmittance at high altitude. In the second assumption, the measurement at larger elevation angle is used for estimation of the critical value of the smaller one. In other words, we assume uniform atmosphere at the same altitude for the measurements of adjacent elevations. If atmospheric conditions changes rapidly or are

localized, it is impossible to estimate the α because of this assumption.

In the Telescope Array experiment, we expect that no observations will be performed or that the data will be discarded under cloudy conditions or if the atmospheric conditions in the field of view change rapidly. Under these conditions we estimate the observation's duty cycle to be 7~10% at the Utah site. For this reason, the assumptions made in this analysis should be acceptable. Based on these assumptions, we can determine the parameter ' k ' and the critical value.

Figure 8 shows the examples of estimated α as a function of altitude at each zenith angle. As we can see, the atmosphere is almost uniform if there are no clouds. In the lower left panel, a cloud can be seen at around an altitude of 6 km. This cloud obscures the signal from higher altitudes. Since the boundary condition at high altitudes cannot be determined, the absolute value of α cannot be analyzed correctly. Figure 9 shows the results obtained on a very clear night. The atmosphere of this night can be almost explained by pure molecular at high altitude. Also the atmosphere was very uniform as is illustrated. It can be clearly seen that the statistical error is very small at all points. For example, the transmittance between the detector and a 10 km distance in the vertical direction is estimated to be 73.27% with a statistical error of 0.05%. Figure 10 shows the result of measurements taken on the next night. The weather was hazy and the atmosphere was not uniform at lower heights. The transmittance between the detector and 10km in the vertical direction is 57.91% with a statistical error of 0.07%. It takes approximately 20 minutes to measure one azimuthal direction.

6 Systematic Error

The systematic error in the present analysis based on the Klett's method has been investigated using a simple Monte-Carlo simulation [9][10]. In this simulation, the signal profile of back-scattered light is calculated using a simple atmospheric model. The number of Rayleigh-scattered photons follows molecular density only, while Mie scattering is calculated by assuming Mie parameters: scale height H_M , horizontal attenuation length L_M , and back-scatter coefficient β_M . An example of the atmospheric model with typical Mie parameters ($L_M=20\text{km}$, $H_M=1.2\text{km}$, $\beta_M=0.05$) is shown in Figure 11. In this calculation, the laser's elevation angle is assumed to be 10 degrees.

This artificial data is analyzed using the same programs as above, employing real data analysis. In Figure 12, examples of the results are shown. The expected α which is calculated based on the input atmospheric model and the estimated one using Klett's method are compared. In Figure 12.a the

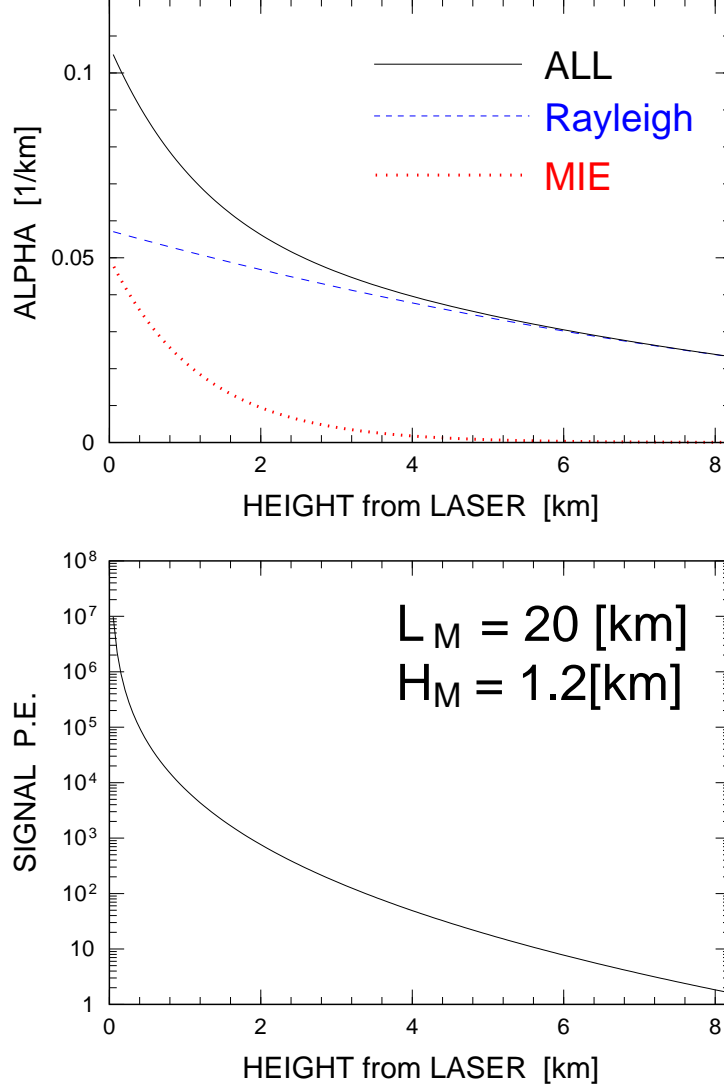


Fig. 11. An example of the atmospheric model used for simulation. Typical Mie parameter values are used for this simulation as indicated in the figure. The diameter of the receiver mirror is 1.5m, laser intensity is 10mJ, and the laser elevation angle is 10 degrees. In the upper panel, dashed and dotted lines indicate the expected α from Rayleigh and Mie scattering, respectively. The solid line indicates the expected α from both types of scattering. The lower panel shows the expected number of photo-electrons detected using LIDAR.

standard atmospheric model is assumed with typical Mie parameters as in the previous figure.

In Figure 12.b, Mie parameters are the same as the standard model except for β_M which is transformed from 0.1 to 0.05 at 2 km height. The Klett's assumption of a power-law relationship between α and β does not take into account variation of the aerosol particle types. If the aerosol particle size is large, forward-scattered light is predominated in Mie scattering. If it is small,

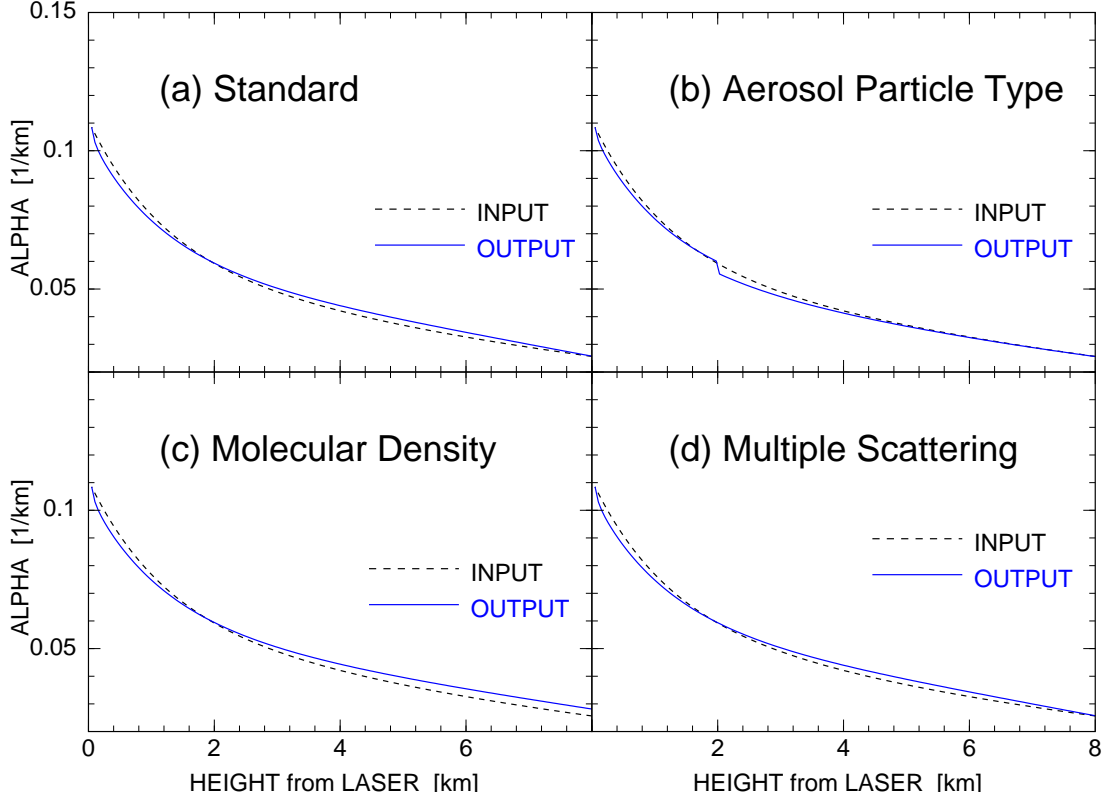


Fig. 12. Examples of results of the simulation. Dashed lines indicate the true value of alpha which is calculated from each atmospheric model. Solid lines indicate the estimated alpha based on Klett's method under the assumption of that alpha is known at the level of the detector. (a) The standard atmospheric model is used as in the previous figure. (b) β_M is changed from 0.1 to 0.05 at 2km height. In this case, the total cross section which is proportional in α is the same as the standard model but the phase function of Mie scattering changes rapidly. (c) Molecular density is overestimated at its highest point. (d) Multiple scattering is considered based on a simple assumption. In this case, 10% of the observed light is assumed to be multiple scattered light. The details of each parameter is in the text.

the phase function of Mie scattering becomes similar to that of Rayleigh scattering. In this panel the total cross section is the same as the standard model, but the phase function of the Mie scattering changes rapidly at 2 km height. The changing of aerosol types can cause significant systematic errors in this analysis as we can see.

In Figure 12.c, all Mie parameters are the same as those of the standard model. But the critical value which is determined based on Rayleigh scattering at the furthest point is assumed to have a 10% systematic error. This critical value is estimated under the assumption that all of the backscattering at the highest point is Rayleigh scattering. In this case, this critical value can be estimated based on molecular density which depends on temperature, pressure and the type of atmospheric model used. In this panel, we assume that the critical

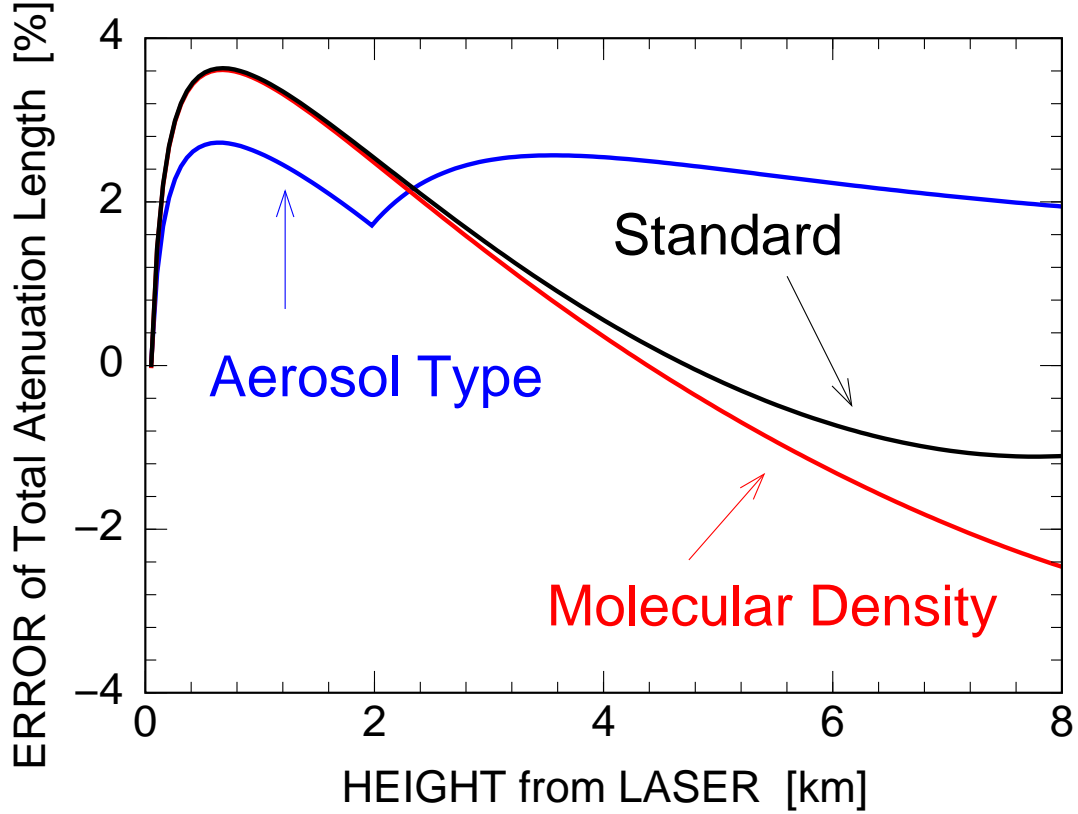


Fig. 13. The systematic error of total attenuation length between the laser and the measurement point as a function of height. The input atmospheric models are the same as in the previous figure.

value is overestimated beyond the true value by 10%. A similar situation can arise when we ignore the effect of Mie scattering to obtain the critical value under an unclear atmosphere.

In Figure 12.d, all Mie parameters are the same as in the standard model. But multiple scattered light is considered under the assumption that 10% of the observed backscattering light is multiple scattered light. A more complete study of the effect of multiple scattering lies outside the scope of this paper. There is no effect to the estimated value under this simple model.

Figure 13 shows the systematic error of the total attenuation length between the laser and measurement point as a function of height. According to these figures, the systematic error caused by Klett's method is less than 5% at all of the measurement points in the standard atmospheric mode. Most significant effect is caused by variation of the aerosol type. These systematic errors should be dependent on the laser's elevation angle, the Mie parameters, and the type of atmospheric model used. Further investigation of the simulation study is described in [10][11].

The detector constants (for example: mirror reflectivity, PMT gain, beam intensity, and so on) do not contribute to the systematic errors in this analysis except for the linearity of the PMT. The effect of multiple scattering is ignored in this measurement. The most significant systematic error is caused by the uncertainty of the critical value. The altitude of 10 km, where we established the boundary condition, may not be high enough to ignore the effect of Mie scattering. This problem can be solved if we use a larger mirror or a higher intensity laser.

7 Summary

We have developed a steerable LIDAR system for atmospheric monitoring by the Telescope Array. The system consists of a 5 mJ pulse laser and 16 cm diameter mirror. Using this system, a technique for atmospheric monitoring was developed.

First, the extinction coefficient α at the level of the detector is measured. Then α is estimated at all directions using Klett's method. The transmittance of the night sky to a distance of more than 10 km can be measured successfully. The statistical error in this analysis is less than 2% under a clear sky. It takes approximately 20 minutes to measure one azimuthal direction.

The systematic error which is caused by this method of analysis is estimated to be approximately 0.5% in a typical atmospheric model. The detector constants do not contribute to the systematic errors in this analysis except for the linearity of the PMT. The most significant systematic error is caused by uncertainty of the critical value and variation of the aerosol type. Some of these problems can be solved if we use a larger mirror or a higher intensity laser.

Based on these observational results, we are considering future plans regarding atmospheric monitoring for the Telescope Array. The signal to noise ratio is in proportion to beam intensity, mirror diameter, square root of observation time, and transmittance. $5mJ \times 16cm \times \sqrt{20min} = 358[mJ \cdot cm \cdot min^{1/2}]$ is required to measure to a distance of 10km under a clear sky (in this case, the transmittance is about 60% in the vertical direction). To measure more than 50 km, we need $358 \times 5^2 / 0.6^5 = 115000[mJ \cdot cm \cdot min^{1/2}]$. This means that a 270 mJ laser is necessary for a 3 m diameter mirror if we want to measure one azimuthal direction in 2 minutes. This value can be reduced by a narrow band filter, small field of view, and high altitude location since the main component of the noise is night sky background light. For a telescope with a 1 degree field of view and $F=1$, the observed night sky background is about 5 MHz in the ultraviolet region.

For the operation of the Telescope Array detector, independent and redundant measurements of the atmosphere should be done for the sake of verification and cross-checking. In fact, several measurements being performed by the Telescope Array and the HiRes groups [12][13][14][15][16][17][18]. For example, These include the measurement of the large angle scattered light of a polarized laser beam and radio-controlled xenon flashers using the HiRes detector, monitoring the transmittance of the air around the detector using the Nepherometer, measurement of the zenith angle dependence of star light and so on. By combining these measurements and the LIDAR method, more reliable measurements can be performed in the future.

Acknowledgements

This work is supported by grants in aid #12304012 and #11691117 for scientific research from the JSPS(Japan Society for the Promotion of Science). The authors thank Dr. Lawrence R. Wiencke, Dr. Michael E. Roberts, and Prof. John A.J.Matthews for their thoughtful discussions.

References

- [1] L.R.Wiencke, *et all* : NIM A **428**(1999)593-607
- [2] M.Chikawa, *et all* : Proceedings of the 26th ICRC (1999)OG4.5.17
- [3] R.Gray, *et all* : Proceedings of the 26th ICRC (1999)OG4.5.04
- [4] N.Hayashida, *et all* : Proceedings of the 26th ICRC (1999)OG4.5.05
- [5] J.R.Mumford, *et all* : Proceedings of the 26th ICRC (1999)OG4.5.10
- [6] W.Viezee, J.Oblanas, R.T.H.Collis:SRI report AFCRL-TR-73-0708(1973)
- [7] J.D.Klett : Appl.Optics,**20**(1981)211-220
- [8] F.G.Fernald : Appl.Optics,**23**(1984)652-653
- [9] John A.J.Matthews : private communication(2001)
- [10] John A.J.Matthews : HiRes/Pierre Auger Note GAP-2001-046
- [11] John A.J.Matthews : HiRes/Pierre Auger Note GAP-2001-051
- [12] M.D.Roberts, *et all* : Proceedings of the 27th ICRC (2001)HE1.07
- [13] M.D.Roberts, *et all* : Proceedings of the 27th ICRC (2001)HE139
- [14] M.Sasano, *et all* : Proceedings of the 27th ICRC (2001)HE1.07

- [15] T.Yamamoto, *et all* : Proceedings of the 27th ICRC (2001)HE1.07
- [16] L.R.Wiencke, *et all* : Proceedings of the 27th ICRC (2001)HE140
- [17] M.Chikawa, *et all* : Proceedings of the 27th ICRC (2001)HE144
- [18] R.W.Clay, *et all* : Proceedings of the 27th ICRC (2001)HE143

This figure "10.gif" is available in "gif" format from:

<http://arxiv.org/ps/astro-ph/0208194v1>

This figure "8.gif" is available in "gif" format from:

<http://arxiv.org/ps/astro-ph/0208194v1>

This figure "9.gif" is available in "gif" format from:

<http://arxiv.org/ps/astro-ph/0208194v1>